



The dye removal from aqueous solution using polymer composite films

Fatih Şen¹ · Özkan Demirbaş² · Mehmet Harbi Çalimli³ · Ayşenur Aygün¹ · Mehmet Hakkı Alma⁴ · Mehmet Salih Nas⁴

Received: 8 August 2018 / Accepted: 16 October 2018 / Published online: 25 October 2018
© The Author(s) 2018

Abstract

The composite consisted of clay and polymers like polyethylene (GCP) was used to remove methylene blue (MB) from the water. The most effective pH, temperature and initial dye concentration in adsorption process were found to be 9, 55 °C and 5×10^{-6} M, respectively. The results of the experiment showed that the adsorption process was compatible with the pseudo-second-order model. Activation parameters of ΔG : -70.64 K J mol⁻¹, ΔS : -70.64 J mol⁻¹ K⁻¹, E_a : 12.37 K J mol⁻¹ at 308 °C were calculated and showed that adsorption process was exothermic and spontaneous. The results revealed that adsorption of MB on composite GCP was spontaneous and the composite of GCP_f could be used for removing of MB from the water.

Keywords Adsorption · Composite film · Polyethylene · Thermodynamic parameters

Introduction

Nanotechnology and nanomaterials are being used for various applications such as organic reactions, solar cells, fuel cells, hydrogen storage, sensors, dye removal applications (Celik et al. 2016; Gezer et al. 2017; Giraldo et al. 2014; Wang et al. 2016; Sahin et al. 2018; Young et al. 2018; Abrahamson et al. 2013; Saravanan et al. 2013a, b, c, d, e, 2015a, b; 2016a, b; Ghaedi et al. 2015; Salunkhe et al. 2016; Mittal et al. 2010; Gupta et al. 2011, 2014a, b, 2015; Mohammadi et al. 2011; Robati et al. 2016; Asfaram et al. 2015; Ahmaruzzaman and Gupta 2011; Khani et al. 2010; Devaraj et al. 2016; Gupta and Saleh 2013; Saleh and Gupta 2011; 2012a,

b; 2014). From these applications, dye removal applications have an important place among them and removal of dyes from water is extremely important (Saravanan et al. 2015a, b; Yang et al. 2018). The increase in dyes pollutants in water is extremely dangerous for the plant, animal and human life (Saravanan et al. 2016a, b; Fan et al. 2012). Because of having a toxic effect on aquatic life and reducing photosynthetic activity of aquatic life by reducing light transmittance, painted wastewater causes significant environmental problems (Barquist and Larsen 2010; Fu and Viraraghavan 2001). Composite materials are generally based on the principle of combining different materials in a particular manner. The ultimate aim to obtain composite material is to allow a new homogeneous material from different properties. Composite materials consist of a combination of matrix and reinforcing elements (Hahn and Gates 1980). Besides, polyethylene is a thermoplastic material which is chemically stable, inexpensive in cost, showing quite high resistance and non-sensitive in low temperatures (Zhano et al. 2005). Generally, methods used to remove harmful substances from the water are adsorption, bio-sorption, ion-exchange, chemical coagulation–flocculation, ozonation, chemical, and photo-oxidation. Specifically, one of the high treatment methods for the treatment of painted wastewater is adsorption (Kannan and Sundaram 2001; Aksu 2005). Among the mentioned dyes, methylene blue (MB) (3,7-bis(dimethylamino)-fenazotiyony chloride) is a dark blue dye

✉ Fatih Şen
fatihsen1980@gmail.com

✉ Mehmet Salih Nas
mehmet.salih.nas@igdir.edu.tr

¹ Sen Research Group, Department of Biochemistry, Faculty of Arts and Science, Dumlupınar University, Evliya Çelebi Campus, 43100 Kutahya, Turkey

² Department of Chemistry, Faculty of Science and Literature, University of Balıkesir, Balıkesir, Turkey

³ Tuzluca Vocational High School, Iğdir University, Iğdir, Turkey

⁴ Department of Environmental Engineering, Faculty of Engineering, University of Iğdir, Iğdir, Turkey

which is easily soluble in water, ethanol, and chloroform and has the gripping force in water. This dye is a cationic molecule, its molecular weight is 373.9 g mol^{-1} , and it has a $\text{C}_{16}\text{H}_{18}\text{N}_3\text{S}\cdot\text{Cl}\cdot 3\text{H}_2\text{O}$ formula. Because it has a strong adsorption capability, it has been chosen for this study. In this work, it was aimed to remove the MB dye from aqueous solutions using the composite consisted of polyethylene and green clay. Kinetics of adsorption process between the composite and MB, the thermodynamic data such as entropy, Gibbs energy, and enthalpy of the process were evaluated. Samples of natural green clay, polyethylene, and the composite GCP_f were characterized by SEM, BET, and TGA analysis, respectively. With the results of the study, it was found that the obtained composite material could be used effectively to remove pollutants like methylene blue from the water solutions.

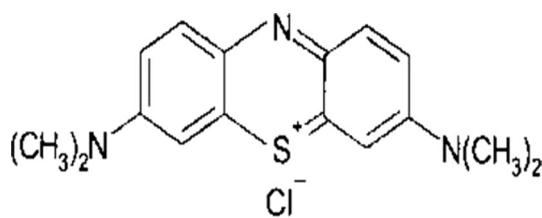
Experimental

Materials

Methylene blue was obtained from Carlo Erba company. Scheme 1 lists chemical formula of methylene blue. Polypropylene (PP) which was used as the matrix at the composite film was obtained from company PETKİM. Green clay used in this study was obtained from the region of Gurpınar (Van-Turkey). The structure of green clay was investigated in scanning electron microscopy (SEM). All the chemicals used in the study are of analytically appropriate quality. BET nitrogen adsorption (Micromeritics Flow Sorb II-2300) was done for finding the effective surface area. Tables 1 and 2 show the contents and some properties of green clay, respectively.

The process of adsorption experiments

The experiments of adsorption were performed by using mechanical stirring. Pure water was used to prepare methylene blue solutions. The experiment was performed with an initial concentration of methylene blue, $1 \times 10^{-5} \text{ M}$, at room temperature with the stirring speed of 600 rpm (pH 9). The solution of methylene blue was agitated for 1440 min



Scheme 1 Chemical structure of methylene blue

Table 1 The content of green clay used in the study

Constituent	Percentage present (%)
Si	44.79
O	36.80
Al	9.20
Mg	20.74
Fe	12.48
Ca	10.02
Others	2.77

at 600 rpm. For the adjusting of the methylene blue solution, NaOH ($5 \times 10^{-2} \text{ M}$) and HCl ($5 \times 10^{-2} \text{ M}$) were used. The kinetic experiments were carried out with 1×10^{-5} , 2.5×10^{-5} , $5 \times 10^{-5} \text{ M}$ of methylene blue solutions, at pH of 5.5, 7, 9 and at various temperatures such as 298, 308, 318, 328 K. 4 mL sample was taken from the main solution for each adsorption analysis. This sample was centrifuged (Cary 1E UV-Vis spectrophotometer) for 5 min at 3000 rpm stirring speed. The remains of the solution were used for adsorption analysis. The adsorption changes were monitored and Eq. (1), as shown below, was used to calculate the amount of adsorbed methylene blue.

$$q_t = [C_0 - C_t] \times V/m \quad (1)$$

where q_t is the amount of initial adsorbent, C_0 is the initial concentration of MB, C_t is the concentration of MB at any time, m is the mass of the composite, and V is the volume of the solution.

Results and discussion

Effect of initial concentration of methylene blue on adsorption rate

The experiments of the GCP_f blend at different methylene blue concentrations with stirring speed of 600 rpm were performed to determine the equilibrium time. Figure 1 shows that when the concentration of the methylene blue was increased, adsorption kinetics also increased. The time

Table 2 Some properties of green clay

Parameters	Value
Grain size (mesh)	325
Color	Green
pH	9.73
Specific surface area (single point)	$148.4 \text{ m}^2 \text{ g}^{-1}$
Specific surface area (single point)	$154.7 \text{ m}^2 \text{ g}^{-1}$

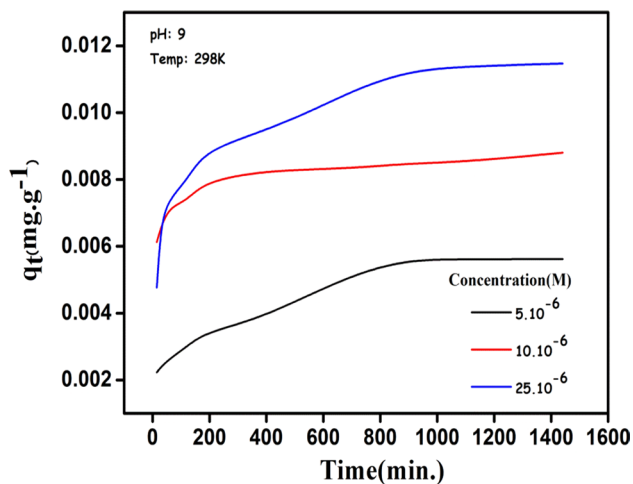


Fig. 1 The change of adsorption kinetics with different methylene blue concentration

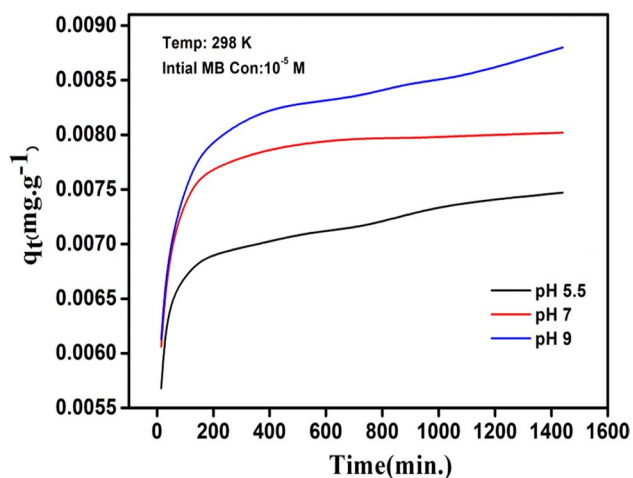


Fig. 2 The exchange of adsorption kinetics with different pH of solution

required to reach a constant concentration according to Fig. 1 is about 800–1000 min.

The exchange of adsorption kinetics with different pH of the solution

The exchange of adsorption kinetics with different pH of the solution is given in Fig. 2. As the pH increased, the adsorption kinetics increased. Generally, adsorbents used in adsorption studies have both negative and positive charges (Burns et al. 1979; Treybal 1963; Nandi et al. 2009). The green composite polyethylene (GCP) used in the study has both positive and negative charges on its surface. These charged particles affect the OH^- ions in the solution medium. The removal of methylene blue (MB) from water solution was

found to be effective at range pH of 5.5–9. This can be attributed to the hydrophobic functional groups (originating from polyethylene) present on the surface of the GCP composite material (Ghaedi et al. 2011). This situation can express that when the pH value of the solution increases, the formation of strong electrostatic forces occurred between the positively charged MB and the negatively charged GCP_f composite film (Li et al. 2010; Lim et al. 2015). The formation of GCP_f composite material and the removal of MB dye from water solution are summarized in Scheme 2 and shown in Fig. 3.

The exchange of adsorption kinetics with various temperature of solution

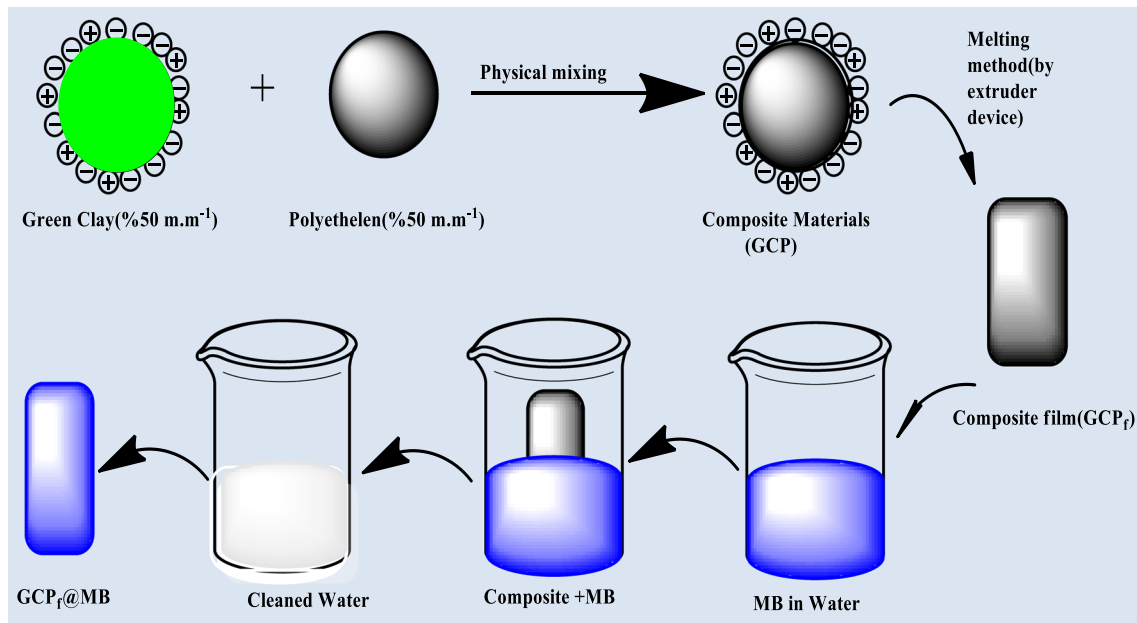
Figure 4 shows the exchange of adsorption kinetics with a variable temperature of the solution. It was seen that the temperature was the very effective parameter in MB dye adsorption experiments. These experiments were performed at 25, 35, 45 and 55 °C, with initial methylene blue concentration of 2×10^{-5} M at pH of 9. The highest adsorption value was obtained at 55 °C. The kinetic energy of the molecules increases with increasing temperature. When the temperature of the solution increased, the diffuse of molecules on the surface composite increased and then adsorption was also increased. The pores of composite increase volume with temperature and the adsorption of MB is positively affected (Dahri et al. 2015).

TGA (thermal gravimetric) analysis of materials and/or composites

TGA analysis was carried out with respect to thermal degradation and mass losses of the samples. Perkin Elmer Pyres model analyzer was used for TGA. The green clay was analyzed at a temperature range of 100–700 °C, and the polyethylene was analyzed at a temperature range of 50–450 °C. All TGA analyses were performed at a nitrogen atmosphere and a heating rate of 10 °C/min. TGA analysis is given in Fig. 5. Figure 5a shows that the loss of water in polyethylene started at 100 °C and the loss of water ratio was 3.2%. Figure 5 shows that the composite (b) shows a more stable structure at the temperature range of 0–100 °C than the pure green clay sample. The situation in other temperatures can be interpreted that mass loss occurs due to the separation of some functional groups and deterioration of the structure at the temperature range of 350–450 °C.

SEM analysis of materials and/or composites

SEM images of pure polyethylene (PE), the composite (GCP_f) film consisted of pure polyethylene–green clay and the composite adsorbed methylene blue (GPC_fM) are given in Fig. 6. Figure 6a shows the SEM image of pure



Scheme 2 Formation of GCP_f and its removal MB from water solution

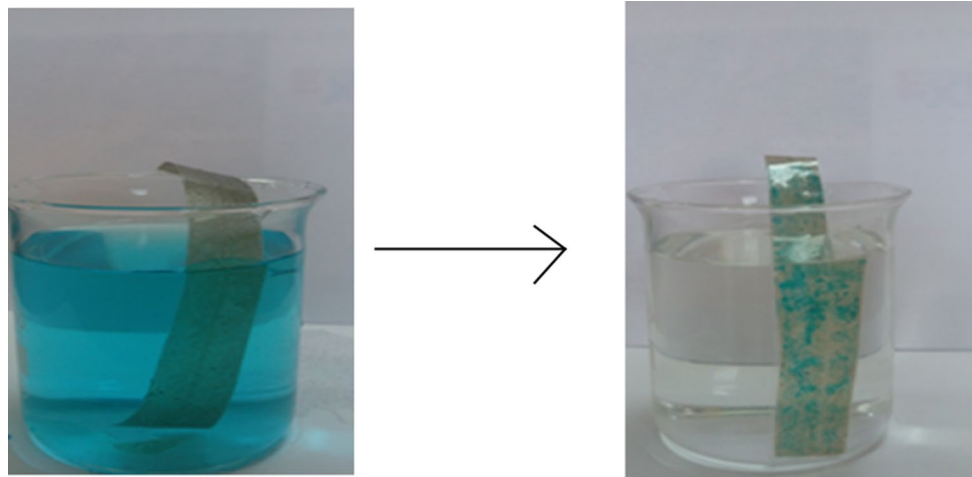


Fig. 3 Removal of MB from water in the laboratory

PE and as shown here, some porous structure is seen on the surface PE. Figure 6b indicates the surface of GCP_f. Bright and dark dots are seen on the surface of the composite. These dots show both polyethylene and green clay. In Fig. 6c, the methylene blue absorbed by the composite material can be clearly visible. After the adsorption, the composite surface appears brighter and smoother. This situation indicates that the composite material is covered with the MB.

Investigation of suitable adsorption kinetic models

Three models were investigated to find the suitable model for the interaction between the composite material and the dye. These models are the pseudo-first-order model, pseudo-second-order model, mass transfer and intra-particle diffusion models. Tables 3 and 4 show the results of experiments and calculated values of models for the adsorption process.

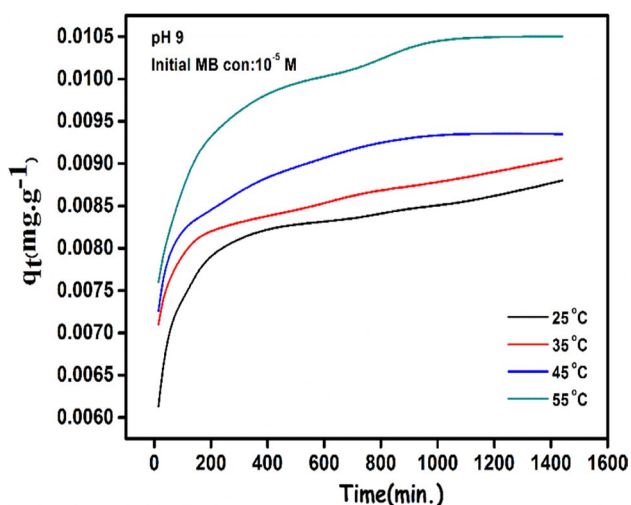


Fig. 4 The exchange of adsorption kinetics with a various temperature of solution

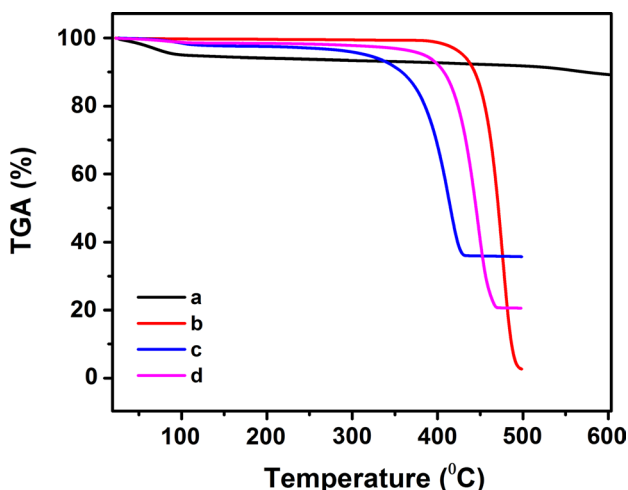


Fig. 5 TGA diagram of pure green clay (a), pure polyethylene (b), green clay + polyethylene (composite) (c), green clay + polyethylene + methylene blue (d)

Equation (2) is used to find values of the pseudo-first-order model (Demirbas and Nas 2016). Equation (3) shows the pseudo-second-order model. The half-life time of the adsorbing kinetic is shown in Eq. (4). The first rate of adsorption is shown by Eq. (5). In this equations, q_e and q_t represent, respectively, equilibrium time and at any time amount of adsorption dye. k_1 and k_2 are rate constants, and t is time (min.). These two values were found from the plot of $\ln(q_e - q_t)$ (Demirbas and Nas 2016; Laidler and Meiser 1999) with time, respectively, 0.87 and 0.96. $t_{1/2}$ expresses the half-time of the process. Equation (6) was used for calculation of intra-particle diffusion model (Demirbas and Nas 2016). In this equation, k_{int} ($\text{mg (g min}^{-1/2})^{-1}$) is a rate constant of diffused intra-particle

which was calculated from the slope of the graphic in Fig. 3 and calculated values k_{int} are given in Table 4. q_t is the amount of adsorbed methylene blue. Previous studies (Demirbas and Nas 2016; Ho and McKay 1997) showed that the graph of q_t versus $t_{1/2}$ is multi-linear. Thus, similar adsorption events can be characterized by two or more steps.

$$\ln(q_e - q_t) = \ln q_e - k_1 t \tag{2}$$

$$\frac{t}{q_t} = \frac{t}{q_e} + \frac{1}{k_2 q_e^2} \tag{3}$$

$$t_{1/2} = \frac{1}{k_2 q_e} \tag{4}$$

$$h = k_2 q_e \tag{5}$$

$$q_t = k_{int} t_{1/2} + C \tag{6}$$

As it can be seen in Fig. 7, the adsorption phenomenon takes place in two phases. The adsorption event occurred according to the initial linear portion in 12–13 min; after this period, the process will occur according to the second linear portion. The first curve in the graph shows rapid adsorption, while the second curve shows that adsorption was slowed by pore filling. It can be said that the adsorption was compatible with pseudo-second-order according to values of R^2 in Table 3. The calculated values $k_{int,1}$ and $k_{int,2}$ at different conditions are given in Table 4. In Table 4, it is found that $k_{int,1}$ values are higher than $k_{int,2}$. The slope of the graph corresponding to the second linear model is expressed as intra-particle diffusion ($k_{int,2}$ ($\text{mg/(g min}^{1/2})$)) (Dogan and Alkan 2003). The graph between $\ln[(C_0/C_t) - 1/(1 + mK)]$ and t (time) is not linear. In this case, the adsorption phenomenon does not match the mass transfer (Kannan and Sundaram 2001; Nas et al. 2017). The calculated values R^1 and R^2 (regression coefficients) are given in Table 4.

Equation (7) and the slope of Fig. 8 were used to find E_a (J mol^{-1}) (activation energy) in which k_2 is rate constant for the second-order model, R_g is constant gas ($8.314 \text{ J K}^{-1} \text{ mol}^{-1}$), and A is Arrhenius factor. By using the slope of Fig. 8, the activation energy was found to be $12.37 \text{ K J mol}^{-1}$. Activation energy values are smaller than 40 K J mol^{-1} . Therefore, the adsorption process considered to be physical interactions. However, interactions between the activation energy values of $40\text{--}800 \text{ K J mol}^{-1}$ are considered as chemical (Ho and McKay 1997). Equations (8) and (9) were used for calculation of the Gibbs free energy (ΔG), enthalpy (ΔH) and entropy (ΔS). In these equations, the Boltzmann constant ($1.3807 \times 10^{-23} \text{ J K}^{-1}$) is k_B , the Planck constant ($6.6261 \times 10^{-34} \text{ J s}^{-1}$) is h . The other expressions are given in the previous rows.

$$\ln k_2 = \ln A - \frac{E_a}{R_g T} \tag{7}$$

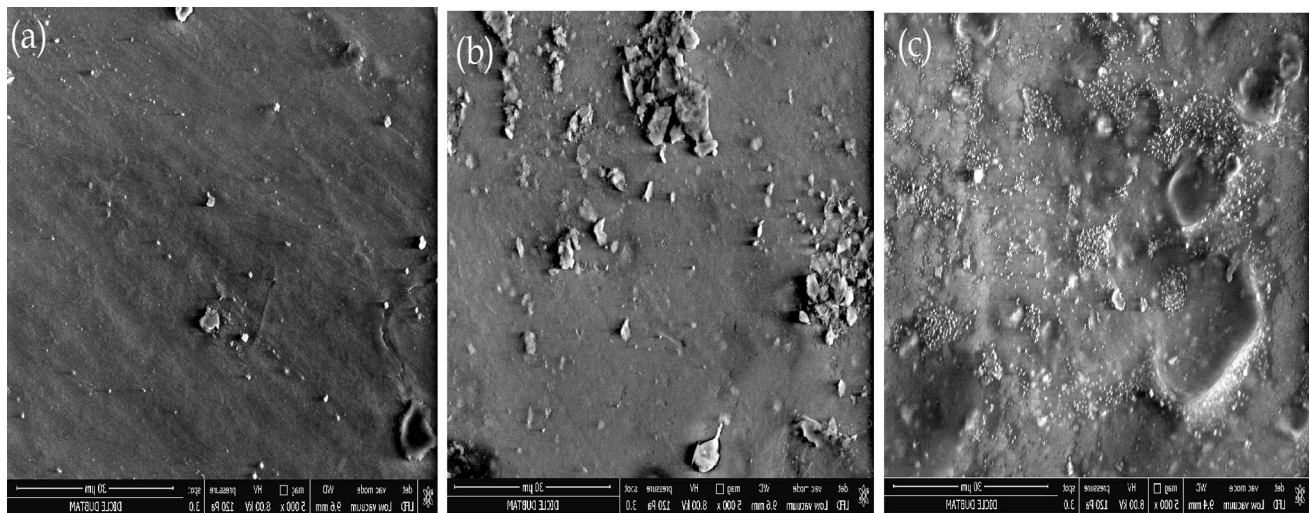


Fig. 6 SEM images of pure polyethylene (a), polyethylene with GC (b) and the composite with methylene blue (c)

Table 3 Calculated kinetic models and some results of experiments

Kinetic models				Pseudo-first-order				Pseudo-second-order		
Parameters				R^2	q_e (calculated)	q_e (exp.) (mg g^{-1})	k_2	R^2	h	$t^{1/2}$
Temp. (K)	Initial dye conc. (g L^{-1}) 10^4	pH	Stirring speed (rpm)							
298	0.1	9	600	0.88	0.0088	0.0088	5.992	0.99	0.0527	3.87
308	0.1	9	600	0.94	0.0090	0.0090	6.127	0.99	0.0551	5.47
318	0.1	9	600	0.95	0.0097	0.0094	8.228	0.99	0.0773	7.45
328	0.1	9	600	0.96	0.0105	0.0105	4.7367	0.99	0.0497	10.95
298	0.05	9	600	0.87	0.0059	0.0059	1.662	0.98	0.0095	13.42
298	0.1	9	600	0.92	0.0085	0.0085	6.0671	0.99	0.0516	18.97
298	0.2	9	600	0.96	0.0117	0.0117	1.7841	1.00	0.0209	23.23
298	0.1	5.5	600	0.92	0.0074	0.0074	9.4500	0.99	0.0699	26.83
298	0.1	7	600	0.91	0.0080	0.0080	15.978	0.99	0.1278	30.00
298	0.1	9	600	0.92	0.0085	0.0085	6.0671	0.99	0.0516	32.86

Table 4 Calculated kinetic models and some results of experiments

Mechanism of adsorption									
Parameters			Mass transfer intra-particle diffusion						
Temp. (K)	Initial dye conc. (g L^{-1}) 10^4	pH	Stirring speed (rpm)	R^2	$k_{\text{int},1}$ ($\text{mg g}^{-1} \text{min}^{-1/2}$) 10^2	R^2_1	$k_{\text{int},2}$ ($\text{mg g}^{-1} \text{min}^{-1/2}$) 10^2	R^2_2	R^2
298	0.1	9	600	0.65	0.0173	0.95	0.0032	0.96	
308	0.1	9	600	0.76	0.0141	0.85	0.0042	0.97	
318	0.1	9	600	0.78	0.0126	0.95	0.0052	0.95	
328	0.1	9	600	0.71	0.0192	0.99	0.0047	0.95	
298	0.05	9	600	0.83	0.0124	0.98	0.0032	0.55	
298	0.1	9	600	0.78	0.0109	0.93	0.0042	0.97	
298	0.2	9	600	0.81	0.0203	0.99	0.0100	0.91	
298	0.1	5.5	600	0.62	0.0145	0.87	0.0024	0.98	
298	0.1	7	600	0.48	0.0166	0.93	0.0013	0.84	
298	0.1	9	600	0.78	0.0109	0.93	0.0042	0.97	

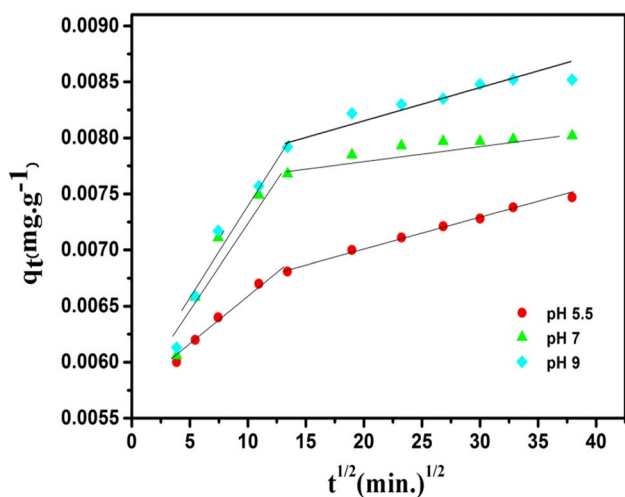


Fig. 7 The plot of intra-particle diffusion for different values of pH

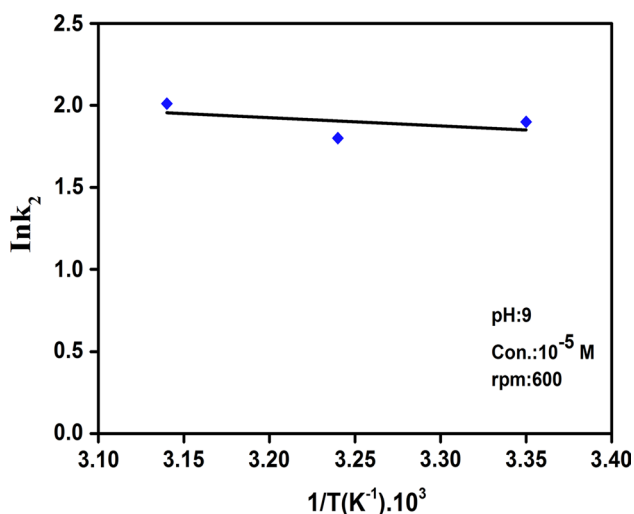


Fig. 8 The plot of $\ln k_2$ versus to $1/T$

$$\ln \left(\frac{k_2}{T} \right) = \ln (k_B/h) + \frac{\Delta S^\circ}{R_g} - \frac{\Delta H^\circ}{R_g T} \tag{8}$$

$$\Delta G^\circ = \Delta H^\circ - T \Delta S^\circ \tag{9}$$

The ΔH was calculated to be $-9.81 \text{ K J mol}^{-1}$ according to Eq. (8). The enthalpy of the process of adsorption is

negative, and physical bonds have taken place between the composite and methylene blue. The calculated values of ΔG and ΔS are seen in Table 5 as negative. These values imply the process of adsorption is spontaneously (Hunter 1999; Mall and Upadhyay 1995).

Conclusions

To conclude, composites film which consists of polyethylene and green clay was successfully formed and performed for methylene blue removal applications. Kinetic parameters of the adsorption between composite and methylene blue were investigated. Temperature, the initial concentration of methylene blue and pH were taken as kinetic parameters. The values initial concentration of methylene blue was 5×10^{-6} , 10×10^{-6} and $25 \times 10^{-6} \text{ M}$, the values of reaction temperature were 25, 35, 45 and $55 \text{ }^\circ\text{C}$, and the values of pH were 5.5, 7 and 9. Experimental results showed that the adsorption increased with increasing methylene blue concentration. It was also observed that the adsorption increased with the increase in the pH values from 5.5 to 9. It was also seen that adsorption increased with increasing temperature because of the increased kinetic energies of the molecules. Four models (pseudo-first-order model, pseudo-second-order model, mass transfer and intra-particle diffusion models) were tried to find the fitting kinetic model of adsorption. According to the results of the experiment, the adsorption of GPC_fM corresponds to the pseudo-first-model for the first 12–13 min, and for the next time period, it corresponds to the second-order model. Thermodynamic parameters were investigated and calculated according to the results of experiments and equations. Thermodynamic parameters showed that the adsorption event is spontaneous, physical and required low energy. It was shown that the obtained composite material film separated methylene blue easily and spontaneously from the water.

Open Access This article is distributed under the terms of the Creative Commons Attribution 4.0 International License (<http://creativecommons.org/licenses/by/4.0/>), which permits unrestricted use, distribution, and reproduction in any medium, provided you give appropriate credit to the original author(s) and the source, provide a link to the Creative Commons license, and indicate if changes were made.

Table 5 Thermodynamic parameters of the MB adsorption

$T \text{ (K)}$	$\Delta G^\circ \text{ (K J mol}^{-1}\text{)}$	$\Delta H^\circ \text{ (K J mol}^{-1}\text{)}$	$\Delta S^\circ \text{ (J mol}^{-1} \text{ K}^{-1}\text{)}$	$E_a \text{ (K J mol}^{-1}\text{)}$
298.0	-68.67	-9.81	-197.51	12.37
308.0	-70.64			
318.0	-72.62			
328.0	-74.59			

References

- Abrahamson JT, Sen F, Sempere B et al (2013) Excess thermopower and the theory of thermopower waves. *ACS Nano* 7(8):6533–6544
- Ahmaruzzaman M, Gupta VK (2011) Rice husk and its ash as low-cost adsorbents in water and wastewater treatment. *Ind Eng Chem Res* 50(24):13589–13613
- Aksu Z (2005) Application of biosorption for the removal of organic pollutants: a review. *Process Biochem* 40:997–1026
- Asfaram A, Ghaedi M, Agarwal S, Tyagib I, Gupta VK (2015) Removal of basic dye Auramine-O by ZnS:Cu nanoparticles loaded on activated carbon: optimization of parameters using response surface methodology with central composite design. *RSC Adv* 5:18438–18450
- Barquist K, Larsen SC (2010) Chromate adsorption on bifunctional, magnetic zeolite composites. *Microp Mesop Mater* 130:197–202
- Burns GP, Lynn S, Hanson DN (1979) Energy reduction in phenol recovery systems. Lawrence Berkeley Laboratory; Report no.: LBL 9176
- Celik B, Kuzu S, Erken E et al (2016) Nearly monodisperse carbon nanotube furnished nanocatalysts as highly efficient and reusable catalyst for dehydrocoupling of DMAB and C1 to C3 alcohol oxidation. *Int J Hydrogen Energy* 41:3093–3101
- Dahri MK, Kooh MRR, Lim LBL (2015) Application of *Casuarina equisetifolia* needle for the removal of methylene blue and malachite green dyes from aqueous solution. *Alex Eng J* 54:1253–1263
- Demirbas O, Nas MS (2016) Kinetics and mechanism of the adsorption of methylene blue from aqueous solution onto Turkish Green Clay. *Acta Curr Int* 6(3):1–10
- Devaraj M, Saravanan R, Deivasigamani RK, Gupta VK, Gracia F, Jayadevan S (2016) Fabrication of novel shape Cu and Cu/Cu₂O nanoparticles modified electrode for the determination of dopamine and paracetamol. *J Mol Liq* 221:930–941
- Doğan M, Alkan M (2003) Adsorption kinetics of methyl violet onto perlite. *Chemosphere* 50:517–528
- Fan L, Luo C, Sun M, Li X, Lu F, Qiu H (2012) Preparation of novel magnetic chitosan/graphene oxide composite as effective adsorbents toward methylene blue. *Bioresour Technol* 114:703–706
- Fu Y, Viraraghavan T (2001) Fungal decolorization of dye wastewaters: a review. *Bioresour Technol* 79:251–262
- Gezer B, Onal Okyay T, Bozkurt S et al (2017) Reduced graphene oxide (rGO) as highly effective material for the ultrasound assisted boric acid extraction from ulexite ore. *Chem Eng Res Des* 117C:542–548
- Ghaedi M, Hossainian H, Montazerzohori M, Shokrollahi A, Shojaiipour F, Soylak M, Purkait MK (2011) A novel acorn based adsorbent for the removal of brilliant green. *Desalination* 281:220–233
- Ghaedi M, Hajjati S, Mahmudi Z, Tyagi I, Agarwal S, Maity A, Gupta VK (2015) Modeling of competitive ultrasonic assisted removal of the dyes—methylene blue and Safranin-O using Fe₃O₄ nanoparticles. *Chem Eng J* 268:28–37
- Giraldo JP, Landry MP, Faltermeier SM et al (2014) A nanobionic approach to augment plant photosynthesis and biochemical sensing using targeted nanoparticles. *Nat Mater* 13:400–408
- Gupta VK, Saleh TA (2013) Sorption of pollutants by porous carbon, carbon nanotubes and fullerene—an overview. *Environ Sci Pollut Res* 20(5):2828–2843
- Gupta VK, Jain R, Nayak A, Agarwal S, Shrivastava M (2011) Removal of the hazardous dye—tartrazine by photodegradation on titanium dioxide surface. *Mater Sci Eng C* 31(5):1062–1067
- Gupta VK, Atar N, Yola ML, Ustundag Z, Uzun L (2014a) A novel magnetic Fe@Au core-shell nanoparticles anchored graphene oxide recyclable nanocatalyst for the reduction of nitrophenol compounds. *Water Res* 48:210–217
- Gupta VK, Nayak A, Agarwal S, Tyagi I (2014b) Potential of activated carbon from waste rubber tire for the adsorption of phenolics: effect of pre-treatment conditions. *J Colloid Interface Sci* 417:420–430
- Gupta VK, Nayak A, Agarwal S (2015) Bioadsorbents for remediation of heavy metals: current status and their future prospects. *Environ Eng Res* 20:001–018
- Hahn HT, Gates TL (1980) Effect of storage time on the tensile strength of Kevlar 49/epoxy strands. *Compos Technol Rev* 1:12–13
- Ho YS, McKay G (1997) Pseudo-second order model for sorption processes. *Process Biochem* 34:451–465
- Hunter J (1999) Introduction to modern colloid science. Oxford University Press, New York
- Kannan N, Sundaram MM (2001) Kinetics and mechanism of removal of methylene blue by adsorption on various carbons a comparative study. *Dyes Pigment* 51:25–40
- Khani H, Rofouei MK, Arab P, Gupta VK, Vafaei Z (2010) Multi-walled carbon nanotubes-ionic liquid-carbon paste electrode as a super selectivity sensor: application to potentiometric monitoring of mercury ion(II). *J Hazard Mater* 183(1–3):402–409
- Laidler KJ, Meiser JM (1999) Physical chemistry. Houghton Mifflin, New York, p 852
- Li YH, Du QJ, Zhang XD, Wang C, Wang ZH, Xia YZ (2010) Removal of copper from aqueous solution by carbon nanotube/calcium alginate composite. *J Hazard Mater* 177:876–880
- Lim LBL, Priyantha N, Ing HC, Dahri MK, Tennakoon DTB, Zehra DTB, Suklueng M (2015) *Artocarpus odoratissimus* skin as a potential low-cost biosorbent for there removal of methylene blue and methylene violet 2B. *Desalin Water Treat* 53:964–975
- Mall ID, Upadhyay SN (1995) Treatment of methyl violet bearing wastewater from paper mill effluent using low cost adsorbents. *J Indian Pulp Pap Technol Assoc* 7(1):51–57
- Mittal A, Mittal J, Malviya A, Gupta VK (2010) Removal and recovery of chrysoidine Y from aqueous solutions by waste materials. *J Colloid Interface Sci* 344(2):497–507
- Mohammadi N, Khani H, Gupta VK, Amereh E, Agarwal S (2011) Adsorption process of methyl orange dye onto mesoporous carbon material—kinetic and thermodynamic studies. *J Colloid Interface Sci* 362(2):457–462
- Nandi BK, Goswami A, Purkait MK (2009) Adsorption characteristics of brilliant green dye on kaolin. *J Hazard Mater* 161:387–395
- Nas MS, Gür A, Gür T, Yönten V (2017) Exploring thermodynamic and kinetic parameters of immobilized catalase enzyme via adsorption on kril clay. *Desalin Water Treat* 67:1–9
- Robati D, Mirza B, Rajabi M, Moradi O, Tyagi I, Agarwale S, Gupta VK (2016) Removal of hazardous dyes-BR 12 and methyl orange using graphene oxide as an adsorbent from aqueous phase. *Chem Eng J* 284:687–697
- Sahin B, Aygun A, Gunduz H et al (2018) Cytotoxic effects of platinum nanoparticles obtained from pomegranate extract by the green synthesis method on the MCF-7 cell line. *Colloids Surf B* 163:119–124
- Saleh TA, Gupta VK (2011) Functionalization of tungsten oxide into MWCNT and its application for sunlight-induced degradation of rhodamine B. *J Colloid Interface Sci* 362(2):337–344
- Saleh TA, Gupta VK (2012a) Photo-catalyzed degradation of hazardous dye methyl orange by use of a composite catalyst consisting of multi-walled carbon nanotubes and titanium dioxide. *J Colloid Interface Sci* 371(1):101–106
- Saleh TA, Gupta VK (2012b) Synthesis and characterization of alumina nano-particles polyamide membrane with enhanced flux rejection performance. *Sep Purif Technol* 89:245–251

- Saleh TA, Gupta VK (2014) Processing methods and characteristics of porous carbons derived from waste rubber tires: a review. *Adv Colloid Interface Sci* 211:92–100
- Salunkhe RR, Young C, Tang J, Takei T, Die Y, Kobayashia N, Yamauchi Y (2016) A high-performance supercapacitor cell based on ZIF-8-derived nanoporous carbon using an organic electrolyte. *Chem Commun* 52:4764–4767
- Saravanan R, Gupta VK, Prakash T, Narayanan V, Stephen A (2013a) Synthesis, characterization and photocatalytic activity of novel Hg doped ZnO nanorods prepared by thermal decomposition method. *J Mol Liq* 178:88–93
- Saravanan R, Karthikeyan S, Gupta VK, Sekaran G, Narayanan V, Stephen A (2013b) Enhanced photocatalytic activity of ZnO/CuO nanocomposite for the degradation of textile dye on visible light illumination. *Mater Sci Eng C* 33(1):91–98
- Saravanan R, Karthikeyan N, Gupta VK, Thirumal E, Thangadurai P, Narayanan V, Stephen A (2013c) ZnO/Ag nanocomposite: an efficient catalyst for degradation studies of textile effluents under visible light. *Mater Sci Eng C* 33(4):2235–2244
- Saravanan R, Joicy S, Gupta VK, Narayanan V, Stephen A (2013d) Visible light induced degradation of methylene blue using CeO₂/V₂O₅ and CeO₂/CuO catalysts. *Mater Sci Eng C* 33(8):4725–4731
- Saravanan R, Thirumal E, Gupta VK, Narayanan V, Stephen A (2013e) The photocatalytic activity of ZnO prepared by simple thermal decomposition method at various temperatures. *J Mol Liq* 177:394–401
- Saravanan R, Khan MM, Gupta VG, Mosquera E, Gracia F, Narayanan V, Stephen A (2015a) ZnO/Ag/Mn₂O₃ nanocomposite for visible light-induced industrial textile effluent degradation, uric acid and ascorbic acid sensing and antimicrobial activity. *RSC Adv* 5:34645–34651
- Saravanan R, Khan MM, Gupta VK, Mosquera E, Gracia F, Narayanan V, Stephen A (2015b) ZnO/Ag/CdO nanocomposite for visible light-induced photocatalytic degradation of industrial textile effluents. *J Colloid Interface Sci* 452:126–133
- Saravanan R, Khan MM, Gracia F, Qin J, Gupta VK, Arumainathan S (2016a) Ce³⁺-ion-induced visible-light photocatalytic degradation and electrochemical activity of ZnO/CeO₂ nanocomposite. *Sci Rep* 6:31641
- Saravanan R, Sacari E, Gracia F, Khan MM, Mosquera E, Gupta VK (2016b) Conducting PANI stimulated ZnO system for visible light photocatalytic degradation of coloured dyes. *J Mol Liq* 221:1029–1033
- Treybal RE (1963) *Liquid extraction*. McGraw Hill, New York, p 48
- Wang J, Tang J, Ding B, Malgras V, Chang Z, Hao X, Wang Y, Dou H, Zhang X, Yamauchi Y (2016) Hierarchical porous carbons with layer-by-layer motif architectures from confined soft template self-assembly in layered materials. *Nat Commun*. <https://doi.org/10.1038/ncomms15717>
- Yang Q, Ren S, Zhao Q, Lu R, Hang C, Chen Z, Zheng H (2018) Selective separation of methyl orange from water using magnetic ZIF-67 composites. *Chem Eng J* 333:49–57
- Young C, Wang J, Kim J, Sugahara Y, Henzie J, Yamauchi Y (2018) Controlled chemical vapor deposition for synthesis of nanowire arrays of metal-organic frameworks and their thermal conversion to carbon/metal oxide hybrid materials. *Chem Mater* 30(10):3379–3386
- Zhano C, Qin H, Gong F, Feng M, Zhang S, Yang M (2005) Mechanical, thermal and flammability properties of polyethylene/clay nanocomposites. *Polym Degrad Stab* 87:183–189

Publisher's Note Springer Nature remains neutral with regard to jurisdictional claims in published maps and institutional affiliations.